

# Simultaneous Voltammetric Comparisons of Reduction Potentials, Reactivities, and Stabilities of the High-Potential Catalytic States of Wild-Type and Distal-Pocket Mutant (W51F) Yeast Cytochrome *c* Peroxidase

Madhu S. Mondal,<sup>†</sup> David B. Goodin,<sup>\*,‡</sup> and Fraser A. Armstrong<sup>\*,†</sup>

Contribution from the Inorganic Chemistry Laboratory, Oxford University, South Parks Road, Oxford OX1 3QR, England, and The Scripps Research Institute, 10550 North Torrey Pines Road, La Jolla, California 92037

Received January 20, 1998

**Abstract:** Protein film voltammetry has been used to measure changes in the catalytic redox energetics of cytochrome *c* peroxidase produced by a single mutation in the distal pocket. Wild-type (WT) cytochrome *c* peroxidase adsorbs at a pyrolytic graphite edge electrode from ice-cold dilute succinate buffer, pH 5.4, to give an electroactive film showing a reversible and narrow (two-electron) signal, reduction potential 754 mV, which converts completely to a catalytic wave at a similar potential when low levels of hydrogen peroxide are added. Under the same conditions, the W51F mutant yields a weaker signal at 883 mV which also transforms to a catalytic wave at similar potential, but with amplitude comparable to that of WT. In either case the catalytic rates are very high. The reversible signals observed for each variant therefore correspond to the catalytic redox couple, analogous if not identical to  $\text{Fe}^{\text{IV}}=\text{O}, \text{R}^+/\text{Fe}^{\text{III}}$ , with replacement of tryptophan-51 by phenylalanine causing a substantial increase in reduction potential (destabilization of  $\text{Fe}^{\text{IV}}=\text{O}, \text{R}^+$ ). The W51F variant appears less stable, even in the resting state, but this does not seriously undermine the results. When the two variants are studied in competition, the non-turnover voltammetry is dominated by the greater electroactive coverage of the WT enzyme, whereas peroxide reduction is controlled at all but the highest rotation rates by the more active W51F. The experiment provides a direct comparison of the real (thermodynamic) catalytic efficiencies of redox enzymes, in this case clearly identifying W51F as intrinsically the more active and efficient variant (*higher* reduction rates at *lower* driving force).

## Introduction

Electron-transfer reactions of proteins and their relationship to biochemical function currently provoke intense interest across a wide spectrum of subdisciplines.<sup>1–3</sup> At the forefront of developments are (a) particular protein systems that are structurally well characterized and able to be probed through site-directed mutagenesis and (b) new methods of studying and quantifying the kinetics and energetics of electron transfer.

Cytochrome *c* peroxidase (CcP) is just such an example of a model protein system. This heme-containing enzyme catalyzes the reduction of  $\text{H}_2\text{O}_2$  by two molecules of cytochrome *c*, in a cycle that is quite well understood and involves species that remain to date the best characterized examples of  $\text{Fe}^{\text{IV}}=\text{O}$  in enzymes.<sup>4</sup> In the most widely accepted mechanism, resting-state  $\text{Fe}(\text{III})\text{-CcP}$  reacts with  $\text{H}_2\text{O}_2$  to give an intermediate known

as compound I, which contains two oxidizing equivalents in the form of  $\text{Fe}^{\text{IV}}=\text{O}$  and a tryptophan-191 based protein cation radical.<sup>5–10</sup> Two molecules of cytochrome *c* reduce compound I back to the resting state via the one-electron intermediate compound II.

Protein film voltammetry exemplifies a method able to create new quantitative perspectives on protein redox chemistry.<sup>11–13</sup> Here, protein molecules are adsorbed at a suitable (“friendly”) electrode surface to mono-submonolayer coverage, such that they exhibit both reversible electrochemistry and levels of catalytic or other activities comparable to those measured by

(5) Liu, R. Q.; Miller, M. A.; Han, G. W.; Hahn, S.; Geren, L.; Hibdon, S.; Kraut, J.; Durham, B.; Millett, F. *Biochemistry* **1994**, *33*, 8678–8685 and references therein.

(6) Sivaraja, M.; Goodin, D. B.; Smith, M.; Hoffman, B. M. *Science* **1989**, *245*, 738–740; Houseman, A. L. P.; Doan, P. E.; Goodin, D. B.; Hoffman, B. M. *Biochemistry* **1993**, *32*, 4430–4443. Huyett, J. E.; Doan, P. E.; Gurbiel, R.; Houseman, A. L. P.; Sivaraja, M.; Goodin, D. B.; Hoffman, B. M. *J. Am. Chem. Soc.* **1995**, *117*, 9033–9041.

(7) Roe, J. A.; Goodin, D. B. *J. Biol. Chem.* **1993**, *268*, 20037–20045.

(8) Miller, M. A. *Biochemistry* **1996**, *35*, 15791–15799.

(9) Matthis, A. L.; Vitello, L. B.; Erman, J. E. *Biochemistry* **1995**, *34*, 9991–9999.

(10) Nocek, J. M.; Zhou, J. S.; DeForest, S.; Priyadarshi, S.; Beratan, D. N.; Onuchic, J. N.; Hoffman, B. M. *Chem. Rev.* **1996**, *96*, 2459–2489.

(11) Armstrong, F. A.; Butt, J. N.; Sucheta, A. *Methods in Enzymology* **1993**, *227*, 479–500. Armstrong, F. A. *Bioelectrochemistry: Principles and Practice*. In *Bioelectrochemistry of Macromolecules*; Lenaz, G., Milazzo, G., Eds.; Birkhauser Verlag: Basel, Switzerland, 1997; Vol. 5, pp 205–255. Armstrong, F. A.; Heering, H. A.; Hirst, J. *Chem. Soc. Rev.* **1997**, *26*, 169–179.

<sup>†</sup> Oxford University.

<sup>‡</sup> The Scripps Research Institute.

(1) Beratan, D. N.; Onuchic, J. N.; Winkler, J. R.; Gray, H. B. *Science* **1992**, *258*, 1740–1741. Onuchic, J. N.; Beratan, D. N.; Winkler, J. R.; Gray, H. B. *Annu. Rev. Biophys. Biomol. Struct.* **1992**, *21*, 349–377.

(2) Moser, C. C.; Keske, J. M.; Warncke, K.; Farid, R. S. Dutton, P. L. *Nature* **1992**, *355*, 796–802.

(3) Durham, B.; Pan, L. P.; Long, J.; Millett, F. In *Electron Transfer in Biology and the Solid State*; Johnson, M. K., et. al., Eds.; Advances in Chemistry Series; American Chemical Society: Washington, DC, 1990; Vol. 226, pp 181. Millett, F.; Miller, M. A.; Geren, L.; Durham, B. *J. Bioenerg. Biomem.* **1995**, *27*, 341–351.

(4) English, A. M.; Tsapraillis, G. *Adv. Inorg. Chem.* **1995**, *43*, 79–125.

conventional methods. In our studies, the electrode is typically hydrophilic; for example, pyrolytic graphite “edge” (PGE) has weakly acidic oxide functionalities which afford a tolerable level of biocompatibility.<sup>11</sup> The technique enables the chemistry of complex systems ranging from labile Fe–S proteins to multi-centered enzymes to be interrogated in considerable detail,<sup>14–17</sup> revealing activity in the “potential domain”, i.e. as a direct function of potential.<sup>15,16</sup> Protein film voltammetry indeed provides an excellent opportunity to generate active-site redox intermediates and examine their thermodynamic and kinetic properties simultaneously. However, success is subject to critical factors, particularly, minimal changes in the intrinsic catalytic and electron-transfer efficiency of the enzyme upon its adsorption (the extreme case being denaturation) and the state of electronic coupling (“wiring”) with the electrode (which is often assumed, incorrectly, to be poor). In designing experiments to probe these factors, an intriguing proposition is to study the competitive voltammetry of enzymes having almost identical structure but with significantly altered reduction potentials and catalytic activity. This is now made possible with a library of active site mutants of CcP.<sup>6,7,18</sup>

We showed recently that yeast cytochrome *c* peroxidase adsorbs in an electroactive state at a PGE electrode,<sup>17</sup> giving rise to a reversible voltammetric signal (pair of oxidation and reduction peaks) at potentials of >700 mV, which transforms to a catalytic wave upon addition of H<sub>2</sub>O<sub>2</sub>. The peaks for either direction have half-height widths of <85 mV at 4° C and are thus associated with a cooperative two-electron exchange. The implication is that the oxidation product is either compound I or a closely related species having similar catalytic activity and hence that the electrode affords a rapid and reversible non-peroxidic/oxygenic route into highly oxidizing enzymic Fe<sup>IV</sup>=O chemistry, analogous to recent experiments using photogenerated

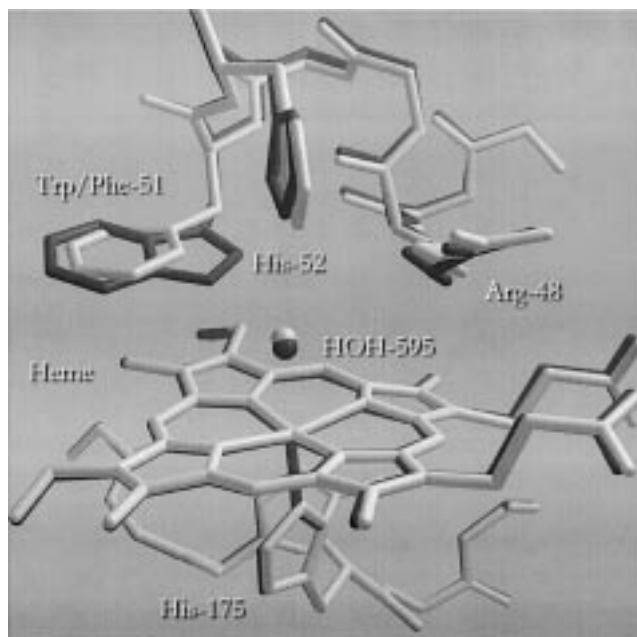


**Figure 1.** Overlaid structures of wild-type and W51F mutant forms of Fe(III) yeast cytochrome *c* peroxidase showing how the Phe ring occupies a position approximately that of the six-membered ring of the original Trp and in the same plane. The distal histidine imidazole undergoes slight twisting (<10°). The distal H<sub>2</sub>O molecule is 2.3 Å above the Fe atom in WT, moving to 2.6 Å in W51F, but these distances vary among all structures determined and cannot be regarded as precise guides. Other changes are insignificant. The structures for WT and W51F were reported previously<sup>23</sup> and coordinates were obtained from the Brookhaven database (entries 1ccp and 4ccp, respectively).

(12) For studies of proteins adsorbed at functionalized alkanethiol monolayers, see: Song, S.; Clark, R. A.; Bowden, E. F.; Tarlov, M. J. *J. Phys. Chem.* **1993**, *97*, 6564–6572. Clark, R. A.; Bowden, E. F. *Langmuir* **1997**, *13*, 559–565. Kasni, A. E.; Wallace, J. M.; Bowden, E. F.; Binet, S. M.; Linderman, R. J. *J. Am. Chem. Soc.* **1998**, *120*, 225–226.

(13) For related studies of proteins immobilized within lipid films, see: Zhang, Z.; Nassar, A. E. F.; Lu, Z. Q.; Schenkman, J. B.; Rusling, J. F. *J. Chem. Soc., Faraday Trans.* **1997**, *93*, 1769–1774. Nassar, A. E. F.; Zhang, Z.; Hu, N. F.; Rusling, J. F.; Kumosinski, T. F. *J. Phys. Chem.* **1997**, *101*, 2224–2231. Hu, N. F.; Rusling, J. F. *Langmuir* **1997**, *13*, 4119–4125. Zhang, Z.; Rusling, J. F. *Biophys. Chem.* **1997**, *63*, 133–146.

(14) Butt, J. N.; Armstrong, F. A.; Breton, J.; George, S. J.; Thomson, A. J.; Hatchikian, E. C. *J. Am. Chem. Soc.* **1991**, *113*, 6663–6670. Butt, J. N.; Niles, J.; Armstrong, F. A.; Breton, J.; Thomson, A. J. *Nat. Struct. Biol.* **1994**, *1*, 427–433. Duff, J. L. C.; Breton, J. L. J.; Butt, J. N.; Armstrong, F. A.; Thomson, A. J. *J. Am. Chem. Soc.* **1996**, *118*, 8593–8603. Butt, J. N.; Fawcett, S. E. J.; Breton, J.; Thomson, A. J.; Armstrong, F. A. *J. Am. Chem. Soc.* **1997**, *119*, 9729–9737.

(15) (a) Sucheta, A.; Ackrell, B. A. C.; Cochran, B.; Armstrong, F. A. *Nature* **1992**, *356*, 362–363. (b) Sucheta, A.; Cammack, R.; Weiner, J.; Armstrong, F. A. *Biochemistry* **1993**, *32*, 5455–5465. (c) Hirst, J.; Sucheta, A.; Ackrell, B. A. C.; Armstrong, F. A. *J. Am. Chem. Soc.* **1996**, *118*, 5031–5038. (d) Hirst, J.; Ackrell, B. A. C.; Armstrong, F. A. *J. Am. Chem. Soc.* **1997**, *119*, 7434–7439.

(16) Heering, H. A.; Weiner, J.; Armstrong, F. A. *J. Am. Chem. Soc.* **1997**, *119*, 11628–11638.

(17) Mondal, M. S.; Fuller, H. A.; Armstrong, F. A. *J. Am. Chem. Soc.* **1996**, *118*, 263–264.

(18) Goodin, D. B.; McRee, D. E. *Biochemistry* **1993**, *32*, 3313–3324; McRee, D. E.; Jensen, G. M.; Fitzgerald, M. M.; Siegel, H. A. and Goodin, D. B. *Proc. Natl. Acad. Sci.* **1994**, *91*, 12847–12851. Fitzgerald, M. M.; Churchill, M. J.; McRee, D. E.; Goodin, D. B. *Biochemistry* **1994**, *33*, 3807–3818. Fitzgerald, M. M.; Trester, M. L.; Jensen, G. M.; McRee, D. E.; Goodin, D. B. *Biochemistry* **1995**, *4*, 1844–1850. Turano, P.; Ferrer, J. C.; Cheesman, M. R.; Thomson, A. J.; Banci, L.; Bertini, I.; Mauk, A. G. *Biochemistry* **1995**, *34*, 13895–13905. Wilcox, S. K.; Jensen, G. M.; Fitzgerald, M. M.; McRee, D. E.; Goodin, D. B. *Biochemistry* **1996**, *35*, 4858–4866. Sun, J.; Fitzgerald, M. M.; Goodin, D. B.; Loehr, J. M. *J. Am. Chem. Soc.* **1997**, *119*, 2064–2065. Musah, R. A.; Goodin, D. B. *Biochemistry* **1997**, *36*, 11665–11673.

Ru(bipy)<sub>3</sub><sup>3+</sup> as an oxidant.<sup>19</sup> The need to extend this line of investigation is made clear by the facts that, with few recent exceptions,<sup>20,21</sup> reduction potential data for heme peroxidases and related oxygenative enzymes are limited to the noncatalytic Fe(III)/Fe(II) couple, and there is little quantitative information on the energetics of catalytically active intermediates involving Fe<sup>IV</sup>=O and radical species.

Here, two peroxidase variants—wild-type (WT) and a mutant W51F in which distal-pocket tryptophan-51 is replaced by phenylalanine—are interrogated by voltammetry. In a novel type of experiment, *both enzymes* are bound at the same PGE electrode and act on the same substrate solution. The mutant is known to be hyperactive as compared to the wild-type enzyme,<sup>7,22–24</sup> while at the same time, it has virtually the same structure.<sup>7,22,23</sup> Figure 1 shows the active site regions of WT and W51F superimposed, from which it can be seen that the only significant difference is that the benzene ring of phenylalanine occupies the center of the space vacated by the indole ring of tryptophan. The experiments simultaneously yield

(19) Berglund, J.; Pascher, T.; Winkler, J. R.; Gray, H. B. *J. Am. Chem. Soc.* **1997**, *119*, 2464–2469.

(20) Farhangrazi, Z. S.; Copeland, B. R.; Nakayama, T.; Amachi, T.; Yamazaki, I.; Powers, L. S. *Biochemistry* **1994**, *33*, 5647–5652.

(21) He, B.; Sinclair, R.; Copeland, B. R.; Makino, R.; Powers, L. S.; Yamazaki, I. *Biochemistry* **1996**, *35*, 2413–2420 and references therein.

(22) Fishel, L. A.; Villafranca, J. E.; Mauro, J. M.; Kraut, J. *Biochemistry* **1987**, *26*, 351–360. Goodin, D. B.; Mauk, A. G.; Smith, M. J. *Biol. Chem.* **1987**, *262* (16), 7719–7724. Miller, P.; DePillis, G. D.; Ferrer, J. C.; Mauk, A. G.; Montellano, P. R. O. *J. Biol. Chem.* **1992**, *267* (13), 8936–8942. Tsprailis, G.; English, A. M. *Can. J. Chem.* **1996**, *74*, 2250.

(23) See: Wang, J.; Mauro, J. M.; Edwards, S. L.; Oatley, S. J.; Fishel, L. A.; Ashford, V. A.; Nguyen-huu, X.; Kraut, J. *Biochemistry* **1990**, *29*, 7160–7173 and references therein.

(24) Goodin, D. B.; Davidson, M. G.; Roe, J. A.; Mauk, A. G.; Smith, M. *Biochemistry* **1991**, *30*, 4953–4962.

quantitative comparisons of the redox and catalytic properties of the two enzymes variants. The results also provide an interesting picture of the factors more generally controlling the electrocatalytic response of enzymes.

### Materials and Methods

Wild-type (WT) and mutant (W51F) forms of CcP(MKT) were obtained as described earlier.<sup>24</sup> Concentrated enzyme solutions prepared by dissolving crystals in buffer were stored as frozen beads in liquid nitrogen. For some experiments, the samples were prepurified by FPLC immediately prior to voltammetry. A mono-Q column was used and the enzyme was eluted with a linear gradient from 20 to 500 mM succinate buffer, pH 5.4, in a total volume of 20 mL, at a flow rate 1.0 mL/min. The concentrations of WT and W51F were determined using the respective extinction coefficients of 101.2 and 121.5  $\text{mM}^{-1} \text{cm}^{-1}$ , respectively, at 408 nm.<sup>7</sup>

All solutions were prepared with Millipore (Milli-Q) deionized water (18  $\text{m}\Omega \text{cm}^{-1}$ ). Experiments were performed in 20 mM sodium succinate buffer prepared by mixing 20 mM sodium succinate and succinic acid (each analytical grade, purchased from Fluka) to attain the desired pH (measured at 0 °C). Concentrations of  $\text{H}_2\text{O}_2$  (BDH, analytical grade) were determined by titration with  $\text{KMnO}_4$ .

Voltammetric experiments were performed using an Autolab electrochemical analyzer (Eco Chemie, Utrecht, The Netherlands) equipped with an analogue scan generator and ADC, in conjunction with an EG &G Model 636 electrode rotator. Most experiments were performed using the digital mode, although tests at various scan rates were conducted using the analogue scan generator. The electrodes and cell used for voltammetry have been described previously.<sup>16</sup> Most experiments were performed at 0 °C using an ice bath, while for temperature-dependent experiments, a cell equipped with a thermostated jacket was used. The saturated calomel electrode (SCE) was contained in a sidearm (linked by Luggin capillary) and held at 20 °C, at which we have assumed a value of 242 mV vs standard hydrogen electrode (SHE).<sup>25</sup> The PGE working electrode (area 0.03  $\text{cm}^2$ ) was polished using an aqueous slurry of  $\text{Al}_2\text{O}_3$  (Buehler: 1  $\mu\text{m}$ ) then sonicated extensively with water. The electrode was then transferred to the cell solution containing peroxidase (typically 0.13  $\mu\text{M}$ ) and held typically at a potential of 842 mV for 10 s while rotating at 50 rpm before cycling. Fourier transform smoothing and baseline corrections were carried out as described previously.<sup>16</sup>

### Results and Discussion

**Voltammetry of WT and W51F Variants under Non-turnover Conditions.** Figure 2 shows the baseline-subtracted voltammetric signals of WT and W51F forms of cytochrome *c* peroxidase adsorbed at a rotating PGE electrode from 20 mM succinate solutions (pH 5.4) containing the enzymes either in pure forms or as quantitative mixtures. Optimum activity for the WT enzyme in cytochrome *c* assays occurs at pH  $\sim$ 5,<sup>24</sup> so the choice of pH is a compromise between optimized conditions and those (pH 6.1) used in our previous study.<sup>17</sup> Identical potential ranges (0.59–1.02 V) were used for each variant to eliminate differences due to electrode surface effects. Wild-type CcP alone (i.e., WT/W51F ratio 1:0) gives a well-defined signal consisting of oxidation and reduction peaks with reduction potential 754 mV and separations of typically  $<22$  mV at 20  $\text{mV s}^{-1}$ . Importantly, the peaks are effectively symmetrical (oxidation and reduction being of similar magnitude) with half-height widths each *less* than 83 mV, the theoretical value for a one-electron process.<sup>26,27</sup> This requires that the reaction is a coupled two-electron exchange, i.e. that transfer of the second electron is closely tied to that of the first<sup>16</sup> and is in agreement with the results published earlier for native yeast enzyme.<sup>17</sup>

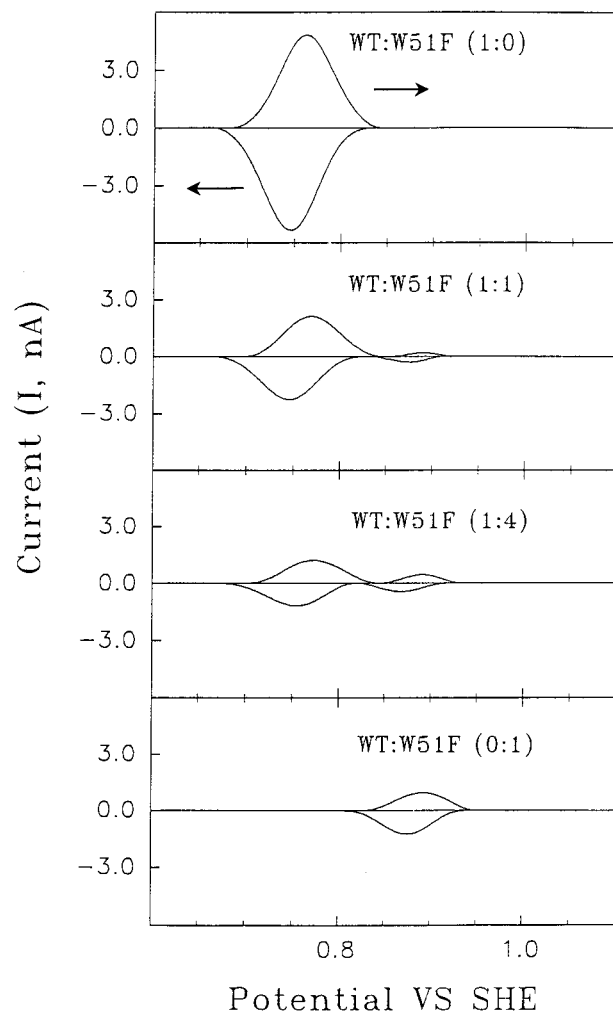


**Figure 2.** Cyclic voltammograms measured for varying solution concentration ratios (1:0, 1:1, 1:4, and 0:1) of WT and W51F cytochrome *c* peroxidase adsorbed at a PGE electrode and contacting 20 mM sodium succinate buffer, pH 5.4. Scan rate: 20  $\text{mV s}^{-1}$ . Temperature: 0 °C. Each voltammogram is the average of four successive cycles, corrected for baseline<sup>16</sup> and Fourier transform smoothed. Arrows indicate direction of scans.

Under these conditions the typical electroactive coverage based on a two-electron reaction is  $2.9 \pm 0.3 \text{ pmol cm}^{-2}$ .<sup>27</sup> By contrast the W51F mutant (i.e., ratio 0:1) shows a signal at the much higher potential of 883 mV. This also consists of symmetrical peaks with narrow half-height widths, but the integrated intensity is reproducibly much lower, typical electroactive coverages being  $0.6 \pm 0.2 \text{ pmol cm}^{-2}$ . The smaller signal from W51F was evident even on the first scan and regardless of the starting potential or the initial poisoning potential (between 0.59 and 1.09 V). Experiments carried out at pH 6.3 (10 mM each of phosphate and succinate buffer) gave similar results but with decreased reduction potential; again, the signal due to W51F (835 mV) was much smaller than that observed for WT (717 mV). The peak widths and their implication for the reduction potentials are discussed further below.

As expected, mixed solutions of WT and W51F showed two independent signals at the expected potentials, but the magnitude

(25) Bard, A. J.; Faulkner, L. R. *Electrochemical Methods; Fundamentals and Applications*; Wiley: New York, 1980.

(26) Plichon, V.; Laviron, E. *J. Electroanal. Chem.* **1976**, *71*, 143–156.

(27) The electroactive coverage of WT was reproducibly lower than reported previously ( $6.2 \text{ pmol cm}^{-2}$ ) for experiments conducted with the native yeast enzyme at pH 6.1. The electroactive coverage is sensitive both to pH and to potential range, the higher switching potential necessary in these experiments giving lower coverage. Half-height widths are higher at pH 5.4 than at pH 6.1. It thus appears that the optimum pH for obtaining voltammetric signals from the enzyme is 6.1.

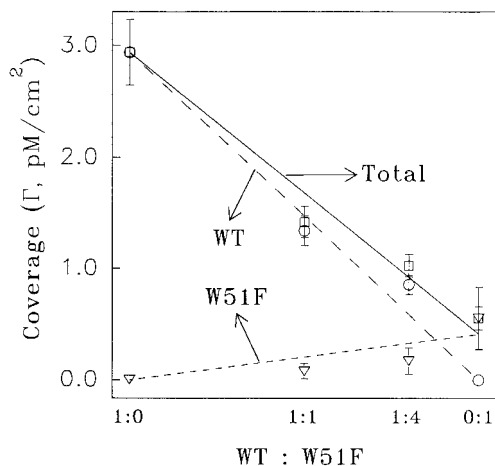


**Figure 3.** Relationship between the electroactive coverages of WT and W51F variants at different solution concentration ratios. Symbols show WT (○, ---), W51F (▽, ---), and total (□, —), with lines indicating the trends of the data points.

in each case was attenuated relative to the 100% experiments, to a degree proportional to the fraction of the other variant present. The combined signal intensity decreases as the ratio WT/W51F is lowered, thus showing that W51F adsorbs with magnitude similar to that of WT but with a large proportion in an electroinactive state. The relationships between signal intensities and solution ratios of WT to W51F enzymes are shown in Figure 3.

Raising the scan rate caused comparable changes in signal appearance and increases in peak separation for WT and W51F, showing that they must have similar interfacial ET kinetics. Over a limited range 20–100 mV s<sup>-1</sup>, the appearance of the signals did not vary significantly, but higher scan rates caused the signals to disappear: measurements were possible only up to approximately 3 V s<sup>-1</sup> for 100% WT, beyond which the signals could not be detected, and up to 0.1 V s<sup>-1</sup> for 100% W51F.<sup>28</sup>

**Catalytic Voltammetry of WT and W51F.** As described previously,<sup>17</sup> introduction of H<sub>2</sub>O<sub>2</sub> to the cell produces a catalytic response from the adsorbed enzymes. Figure 4 shows the voltammograms obtained at various rotation rates for reduction of 5.9 mM H<sub>2</sub>O<sub>2</sub> catalyzed by WT and W51F variants adsorbed from varying solution ratios (1:0, 1:1, and 0:1). Alongside are displayed the derivatives (dI/dE) which reveal the quality and finer details of the data. The immediate observation is that, for the 100% WT and 100% W51F systems, a single catalytic wave is observed which in each case commences just above the respective reduction potentials measured under non-turnover conditions. At lowest rotation rate (50 rpm) H<sub>2</sub>O<sub>2</sub> is clearly depleted from the vicinity of the enzyme, as evidenced from the peak-like ridge observable upon scanning in the negative direction. On raising the rotation rate, these convert to steady-state sigmoidal waves, of increasing limiting current, thus confirming the importance of H<sub>2</sub>O<sub>2</sub> mass transport and showing that the enzymes are very active. By contrast, the 1:1 mixture

(28) These experiments were performed using analogue mode, whereupon observed WT signals were reproducibly more intense than the W51F enzyme. The sharp loss of peak intensity as the scan rate is raised may be due to kinetic decoupling of the two one-electron processes, which would give rise to much weaker and broader independent one-electron signals. Alternatively, gating by coupled chemical reactions could limit the rate of interconversion in the non-turnover reaction. For example, it is known from experiments with horseradish peroxidase that oxidative artificial (non-peroxidative) formation of the Fe<sup>IV</sup>=O group from Fe(III) is limited by a slow step, assumed to be the displacement and binding of the distal water molecule (See ref 19). Similar restrictions may apply in the non-turnover transformations of CcP.

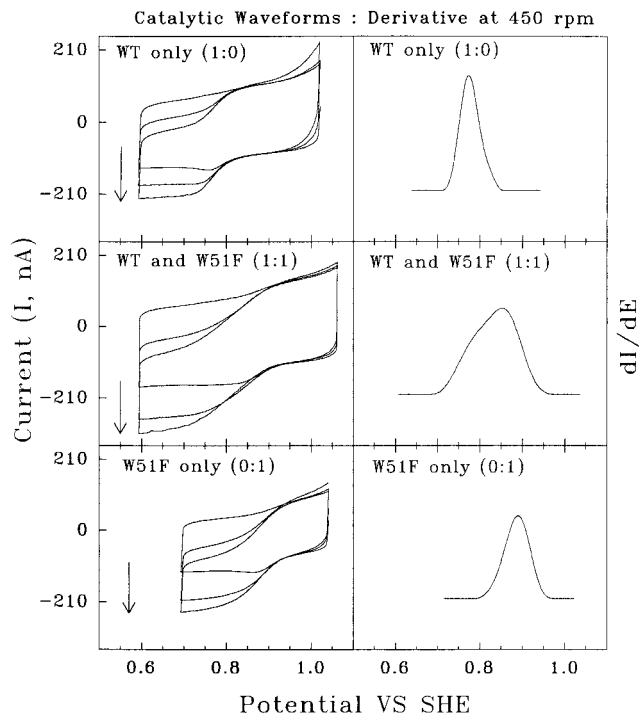


**Figure 4.** (left) Catalytic voltammograms obtained at a rotating PGE disk electrode at which CcP variants are adsorbed from different solution ratios: WT (1:0), mixed (1:1), and W51F (0:1) after introduction of 5.9 mM H<sub>2</sub>O<sub>2</sub> to the cell solution (20 mM succinate buffer, pH 5.4). Scan rate: 20 mV s<sup>-1</sup>. Temperature: 0 °C. The voltammograms in each case show increases in catalytic current with increase in rotation rates (50, 450, and 1250 rpm) indicated by arrows. Limiting catalytic currents for WT-only and W51F-only at the highest rotation rate correspond to rate constants of approximately 1 × 10<sup>6</sup> and 6 × 10<sup>6</sup> M<sup>-1</sup> s<sup>-1</sup>, respectively, using the average surface coverages for each variant. Obviously, catalysis is still largely mass-transport controlled, and so these values are lower than the rate constants given in the text, which are derived from a full Koutecky–Levich and Michaelis–Menten analysis. (right) Derivatives of the catalytic waves measured at 450 rpm.

shows more complex behavior: at the lowest rotation rate a sigmoid is observed close to the potential of W51F, then as the rotation rate is increased the wave broadens, but now to a much greater degree than when a single variant is present. The derivative at 450 rpm reveals the emergence of a second catalytic process, coinciding with lower potential of WT.

To ascertain the catalytic efficiencies of adsorbed WT and W51F we performed experiments for each enzyme at various rotation rates and H<sub>2</sub>O<sub>2</sub> concentrations. The catalytic parameters  $k_{\text{cat}}$  (number of molecules of H<sub>2</sub>O<sub>2</sub> reduced per second) and  $K_M$  were estimated as described previously, using the electroactive coverage to gauge the number of operational enzyme molecules.<sup>17</sup> Thus voltammetric limiting currents were analyzed by the Koutecky–Levich equation, and the resulting catalytic currents (infinite rotation rate) were used in Michaelis–Menten analysis. We obtained (estimated errors in parentheses) for WT,  $k_{\text{cat}} = 407 \text{ s}^{-1}$  (25%) and  $K_M = 118 \mu\text{M}$  (25%), while for W51F,  $k_{\text{cat}} = 3946 \text{ s}^{-1}$  (50%) and  $K_M = 88 \mu\text{M}$  (25%). (Previously, with the native enzyme at pH 6.1, 4 °C, we determined  $k_{\text{cat}} = 268 \text{ s}^{-1}$  and  $K_M = 92 \mu\text{M}$ .<sup>17</sup>) The large errors reflect uncertainties in measuring Koutecky–Levich, Michaelis–Menten limits, and (particularly) for W51F the electroactive coverage. The higher turnover number for W51F reflects the observation that essentially equal electrochemical activity is achieved with a much lower electroactive coverage of enzyme. The apparent second-order rate constants ( $k_{\text{cat}}/K_M$ ) for WT and

W51F at 0 °C are therefore  $3.4 \times 10^6$  and  $4.5 \times 10^7 \text{ M}^{-1} \text{ s}^{-1}$ , respectively.

The catalytic results are readily interpreted in terms of W51F being the most efficient enzyme. Not only does it catalyze  $\text{H}_2\text{O}_2$  reduction at a higher potential (lower driving force) than WT, but the higher limiting current amplitudes show that it also has a higher intrinsic activity. This fact is ensured by the enhancement ratio  $k_{\text{cat}}(\text{W51F})/k_{\text{cat}}(\text{WT})$  of  $\sim 10$ , which lies outside the sizable error margins. Thus, in competitive experiments, W51F dominates the voltammetry under conditions where the catalytic current is controlled by substrate mass transport, i.e. at low  $[\text{H}_2\text{O}_2]$  and low rotation rates. In other words, *all* the peroxide arriving at the electrode is consumed efficiently by the relatively low density of W51F molecules. As the mass-transport limitation is relaxed (e.g., as the rotation rate is raised) WT is able to make an increasing contribution (the shoulder on the negative edge of the “1:1” voltammogram (see Figure 4) diminishes in size as the rotation rate is decreased below 450 rpm).

#### Investigations of the Competition between WT and W51F.

To investigate why W51F gives such a low electroactive coverage and to check the influence of enzyme stability, we carried out further tests. First, experiments were carried out in which  $\text{H}_2\text{O}$  was replaced by a 50% aqueous glycerol mixture. It is known that glycerol protects W51F against formation of an inactive six-coordinate state.<sup>24</sup> However the same low level of non-turnover signal was observed. Second, FPLC experiments showed that both WT and W51F elute at the same salt concentration. To confirm that the two variants are essentially indistinguishable in terms of their overall electrostatic properties, they were mixed in a 1:1 ratio and chromatographed together. A single sharp band eluted at the same position as either of the two components studied individually. Third, the effect of temperature on the catalytic waves was examined to test whether W51F might be the more unstable of the two variants when adsorbed at the electrode. Figure 5 shows voltammograms obtained at 450 rpm,  $5.9 \mu\text{M H}_2\text{O}_2$ , after commencing at 0 °C then scanning at different temperatures up to 34 °C. In each case the catalytic currents decrease irreversibly (i.e., lowering the temperature does not reverse the decline), thus showing that the enzymes become inactivated on the electrode at increasing temperature. The effect is most noticeable with W51F, for which activity was not evident once 34 °C had been reached. For the single-enzyme experiments with WT or W51F, uniform inactivation is observed, with only small alterations in wave shape and potential throughout (see derivatives). However, for the “1:1” film, the first voltammograms at 0 °C are broad yet clearly dominated by W51F; then as the temperature is raised, they transform over to the form expected for WT alone. Variations in the potential range did not significantly affect this observation. A similar result was obtained by allowing films to age at a constant temperature, i.e. 16 °C, thus showing that the changes in voltammetric wave shape are not due to the variants having different activation energies for catalysis.

**General Comments. The Nature of the Non-turnover Redox Transition.** In both cases, the fact that the non-turnover signals observed in the absence of  $\text{H}_2\text{O}_2$  coincide with their respective catalytic potentials provides compelling evidence that the reaction being observed in each case is the reversible transformation between catalytically active redox states. The further observation that for both variants this transformation is a cooperative two-electron process reinforces the conclusion made earlier for the native yeast enzyme.<sup>17</sup> The resting  $\text{Fe(III)}$  state and compound I or its equivalent species are thus

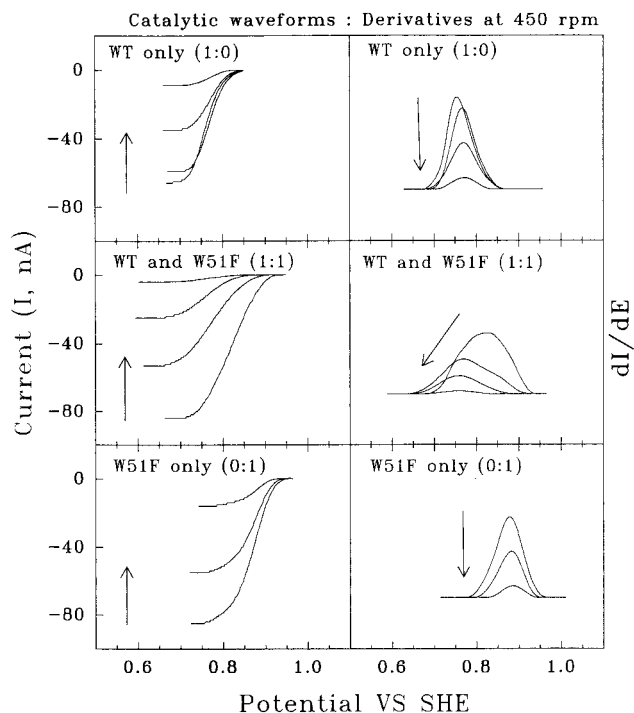
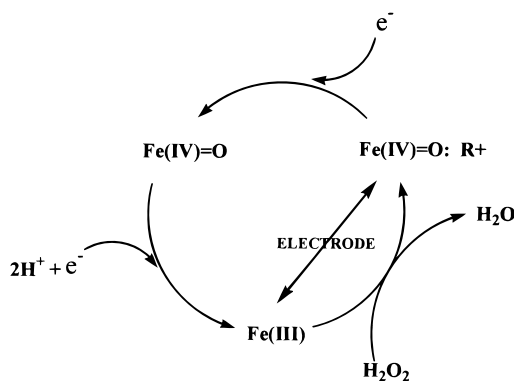


**Figure 5.** Effect of increasing temperature on catalytic voltammograms for CcP-adsorbed PGE electrodes prepared from solution mixtures WT (1:0), mixed (1:1), and W51F (0:1) upon introduction of 5.9 mM  $\text{H}_2\text{O}_2$  to the cell solution (20 mM succinate buffer, pH 5.4). Voltammograms were recorded at  $20 \text{ mV s}^{-1}$  and 450 rpm. The catalytic current decreases as the temperature is raised from 0 °C to 12, 24, and 34 °C. W51F is completely inactive at 34 °C. Arrows indicate direction of increasing temperature.

#### Scheme 1



interconverted by two cooperatively coupled one-electron transfers at potentials  $E_{\text{I}}^{\circ}$  and  $E_{\text{II}}^{\circ}$ .<sup>16,17,26</sup> As shown in Scheme 1, the electrode thereby provides an alternative *shuttle* across the catalytic cycle.

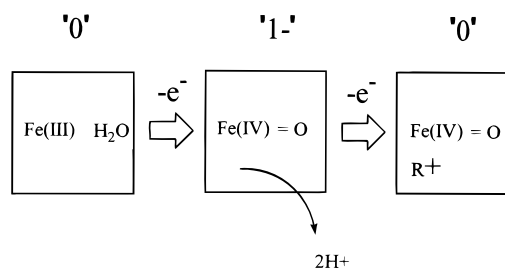
It is likely but not proven that the states involved are identical to the forms generated and characterized in solution, i.e.  $E_{\text{I}}^{\circ}$  = compound I/compound II and  $E_{\text{II}}^{\circ}$  = compound II/ $\text{Fe(III)}$ .<sup>4</sup> Theoretically an ideal one-electron signal shows half-height widths ( $\delta$ ) of 83 mV at 0 °C for each direction.<sup>16,26</sup> Broadening due to dispersion (nonuniform adsorption, potential microenvironments) or anticooperative interactions between redox centers is commonly observed. By contrast, narrowing of the peaks in *both* directions necessitates *cooperative* electron–electron coupling. For example, it can be shown<sup>16,26</sup> that, in the absence of dispersion, two one-electron processes that are coupled (as would be the case if both occur at a single center), measured at 0 °C, will produce  $\delta = 83 \text{ mV}$  (i.e., will appear as

a one-electron signal) when  $E_{I'} - E_{II'} (\Delta E) = 32$  mV. As  $E_{I'} - E_{II'}$  decreases, the signal sharpens, and we obtain, for example,  $\delta = 60$  mV,  $\Delta E = 0$ ;  $\delta = 50$  mV,  $\Delta E = -34$  mV; and (the limiting case for full two-electron cooperativity)  $\delta = 42$  mV,  $\Delta E = \leq -100$  mV. In principle, it should be possible to determine  $\Delta E$ , and thus, both of the one-electron reduction potentials from the peak position and  $\delta$ . In practice, however, only an estimate can be obtained due to the uncertainty in the level of broadening due to dispersion.<sup>29,30</sup> Since  $\delta \leq 74$  mV for either variant, it follows that  $E_{I'} - E_{II'} \leq +24$  mV at pH 5.4. With this limitation considered, points concerning the redox energetics may now be addressed.

The substantial increase in two-electron reduction potential produced by the single mutation (+129 mV at pH 5.4, 118 mV at pH 6.3) gauges the effect of a structurally defined alteration. From the crystal structures of WT and W51F and as summarized in Figure 1, the Fe(III) is five-coordinate in each case, and the distal water molecule (H<sub>2</sub>O-595) appears as a relatively "mobile" group that is probably hydrogen bonded to histidine-52 and W51.<sup>7,22,23</sup> Our attention focuses necessarily on tryptophan-51 and, in particular, in the way in which it can play a central role in the hydrogen bonding network of the distal pocket.<sup>23</sup> In the compound I state, Fe<sup>IV</sup>=O can be stabilized by hydrogen bonding between W51 and the oxene-O atom<sup>4</sup> and it is known that replacement of tryptophan by phenylalanine causes the Fe<sup>IV</sup>=O stretching frequency to increase by 25–30 cm<sup>-1</sup>.<sup>23</sup> Significantly, the amino acid sequence of distal helix B in W51F more closely resembles that of horseradish peroxidase,<sup>31</sup> which also has a much higher two-electron reduction potential, 891 mV at pH 7.<sup>21</sup> Being a two-electron couple (see below) the stabilization afforded to compound I by tryptophan-51 (relative to Phe in the same position) amounts to approximately 25 kJ mol<sup>-1</sup> ( $2 \times 0.129$  F).

Cooperative coupling between the Fe<sup>IV</sup>=O and a nearby organic radical is transpiring to be quite a general characteristic of these enzymes. In particular, the peroxidase from the fungus *Arthomyces ramosus* shows  $E_{I'} = 915$  mV and  $E_{II'} = 982$  mV (i.e.,  $\Delta E = -67$  mV) as measured by equilibration with IrCl<sub>6</sub><sup>3-/2-</sup> at pH 7 and 24 °C.<sup>20</sup> Similar studies with horseradish peroxidase<sup>21</sup> also reveal cooperative coupling, with  $E_{I'} = 879$  mV and  $E_{II'} = 903$  mV (i.e.,  $\Delta E = -24$  mV) at pH 7 and 15 °C. The intermediate, compound II, is therefore best considered as metastable. The simplest mechanism for coupling requires only consideration of the balance of electrostatics in the active site region and is similar to the idea proposed by Powers and co-workers.<sup>21</sup> As depicted in Scheme 2, conversion of the unbound water (H<sub>2</sub>O) to bound oxide (O<sup>2-</sup>) formally releases two protons which must either be bound elsewhere in the active site region or facilitate removal of a second electron.<sup>32</sup>

**Catalytic Activities.** Correcting for electroactive coverage, the voltammetry clearly shows that W51F is the more active variant, as has been noted previously from steady-state solution kinetics.<sup>24</sup> It was found that W51F is approximately 6 times more active than WT using horse heart cytochrome *c* as substrate, yet rates of formation of compound I ( $3.03 \times 10^7$

**Scheme 2**


M<sup>-1</sup> s<sup>-1</sup> for WT vs  $2.2 \times 10^7$  M<sup>-1</sup> s<sup>-1</sup> for W51F<sup>24</sup>) decrease only slightly for W51F. It was therefore suggested that the rate-determining step is reduction of compound I by cytochrome *c*.<sup>24</sup> The voltammetry now shows that the driving forces for oxidation of cytochrome *c* by W51F and WT do indeed differ quite substantially, so that W51F should be the more effective oxidant provided reorganization energies are sufficiently high that the reaction remains in the normal Marcus region. However, our experiments enable the hyperactivity of W51F to be pinpointed more precisely, since unlike the conventional experiment, the potential can be varied continuously to achieve whatever value is required to yield a limiting rate that is independent of driving force. In other words the driving force is conveniently factored out, identifying W51F as the more active variant by a factor of  $\sim 10$ . The hyperactivity of W51F is therefore due to an increase in the intrinsic reactivity of intermediates, i.e. compound I and/or compound II are more labile and break down easily to the resting Fe(III) state.

**Interpretation of Catalytic Wave Forms for Adsorbed Enzyme Films and Gauging Inhomogeneity.** The respective catalytic wave forms provide a simple demonstration of alterations in response to changes in mass-transport control. In each case, the catalytic potentials correlate well with those of the respective non-turnover signals<sup>33</sup> and activity is high, as evidenced immediately from the inability to sustain a steady state at low rotation rates (persistence of peak-like features) and from estimates of the catalytic constants after correcting for coverages. The greater activity of the high-potential W51F variant gives rise to interesting effects in the 1:1 experiment. At low rotation rate, the wave form is dominated by the catalytic action of W51F; however, as the rotation rate is raised to relieve mass-transport control, the catalytic wave spreads down toward negative potentials as WT makes an increasing contribution. This is seen clearly in the derivative which reveals a shoulder at low potential. A related effect is observed when inactivation of the 1:1 system is induced by raising the temperature. The W51F mutant is less stable, so that whereas initially at low temperature it dominates the voltammetry, there is a marked and irreversible shift toward the WT catalytic wave form upon heating. By contrast, the pure enzymes show just a small positive shift (see derivative). This deliberate inactivation experiment shows how it is possible to gauge the homogeneity

(29) Where such cooperativity occurs and where distinctive species are generated, potentiometric titrations offer a better way to define the individual one-electron potentials (see refs 20 and 21). The advantage of voltammetry is that it is a dynamic technique, able to measure reduction potentials under catalytic conditions or where species are only generated as reactive transients.

(30) By comparing our observed  $\delta$  value of 74 mV with the theoretical limit for a fully cooperative two-electron process (i.e., 42 mV at 0 °C), we conclude that dispersion effects must contribute less than ca. 32 mV. This means that the active sites in the enzyme film behave as a homogeneous ensemble.

(31) Welinder, K. G. *FEBS Lett.* **1976**, *72*, 19–23.

(32) The pH dependence of  $E^{\circ'}$  measured for native CcP across the pH range 4.0–8.0 shows a transition from  $2\text{H}^+/2e^-$  to  $1\text{H}^+/2e^-$  with  $\text{p}K_a \sim 6.9$  at 0 °C (Mondal, M. S.; Heering, H. A.; Armstrong, F. A. Manuscript in preparation). Data points for the WT enzyme (measured in the pH range of 5.1–6.6) lie close to and within the error margins of this line. The  $E^{\circ'}$  values for W51F, also measured over the pH range 5.1–6.6, showed a straight line with a negative slope of 51 mV. These results indicate that, for both variants at pH 5.4, the  $\text{H}^+/e^-$  ratio for the transition between resting-state CcP and compound I approaches 1.0, i.e., two H<sup>+</sup> are transferred from the active site upon oxidation.

(33) Detailed interpretation of catalytic wave shapes arising from enzymes adsorbed at electrodes is discussed in the following: Heering, H. A.; Hirst, J.; Armstrong, F. A. Submitted for publication.

of a population of enzyme molecules configured as an electrode surface film: in short, a change in catalytic wave shape upon aging the film should be a good indicator of heterogeneity.<sup>34</sup> The uniform decrease observed for the pure enzymes further shows that inactivation does not proceed through catalytically viable intermediate states operating at different potentials.

**Stability of Adsorbed Enzymes.** The final question concerns why so high a proportion of W51F adsorbs in an electroinactive state. Although it is possible that W51F might be more prone to become adsorbed on the PGE surface in orientations that do not support interfacial electron exchange, our results indicate that the problem lies with its greater instability. The attenuation relative to WT is evident on the first oxidative scan, with the same potential range being used for each variant, thus showing that the electrode potential itself, although expected to be influential, does not provide the reason for the difference in behavior. Neither does the reported instability of W51F compound I appear to pose any serious problem, since in non-turnover experiments, the peak size is not noticeably smaller in the reductive direction as compared to the preceding oxidative scan. It is therefore likely that the inactivation of W51F occurs immediately upon adsorption, perhaps at less accommodating

(34) The complex changes in wave shape accompanying the inactivation of the WT/W51F mixed film may also be contrasted with the catalytic voltammetry of succinate dehydrogenase and fumarate reductase where progressive inactivation produces no change in wave shape. The all-or-nothing "binary" behavior is an indicator of the homogeneity of the adsorbed enzyme sample.

sites on the heterogeneous PGE surface<sup>11</sup> that cause less disruption to a more robust WT enzyme.

## Conclusions

To summarize, protein film voltammetry provides a direct route into ferryl ( $\text{Fe}^{\text{IV}}=\text{O}$ ) chemistry in enzymes, enabling in this case determination of the reduction potentials of highly oxidized states of cytochrome *c* peroxidase variants. The method verifies that these are highly active catalytic states and overcomes problems associated with oxidative degradation that may hinder measurements at such high potentials by conventional titrations. From the results and consideration of structural differences between WT and W51F, the distal pocket residue tryptophan-51 is identified as a major determinant of the compound I/Fe(III) reduction potential, being responsible for a ca. 25 kJ mol<sup>-1</sup> stabilization of compound I. Finally, the systematic variations in voltammetric wave forms, as functions of WT/W51F surface ratio, temperature, and time, all provide interesting insight into the interpretation of catalytic voltammetry by homogeneous as opposed to nonhomogeneous films.

**Acknowledgment.** This research was supported by the United Kingdom EPSRC (Grant GR/J84809 to F.A.A.), by the Wellcome Trust (Grant 042109 to F.A.A.), and by NIH (Grant GM41049 to D.B.G.). We thank Dirk Heering for helpful discussions and Kerensa Heffron, who conducted experiments supplementing the observations we have reported.

JA980197J